Significance of the Level of Excitation on the Nonlinear Response of Medium and Soft Soils

Yoshihiro Sugimura[1)], *Madan B. Karkee[2)], Koji Sato[1)], Xu Ting[1)]

1) *Department of Architecture, Faculty of Engineering, Tohoku University, Japan*
2) *GEOTOP Corporation, Sankyo Building, Nihonbashi, Tokyo, Japan*

ABSTRACT

Nonlinearity due to strong earthquake shaking is a major consideration in the study of local site effect. This aspect of the site effect depends on the level of excitation, as well as on the soil conditions. In addition, the nonlinear response depends on the period and phase contents of the incident motion. In this study, three levels of incident excitations, represented by the respective response spectra, are utilized to investigate the nonlinear response of medium and soft site conditions. The results show that the response can be substantially influenced by long period components in the incident motion, owing to the significant elongation in ground period. The effect is dominant in medium and soft sites. Various nonlinear ground response characteristics are discussed in this context.

INTRODUCTION

The range of applicability of the ground response characterization based on the low strain soil properties, is determined by the rate of strength degradation with increasing strain. Most of the soil types encountered in urban areas in Japan [7] are found to begin exhibiting strength degradation at fairly low strain levels. Consequently, nonlinearity during large earthquakes can be expected to be substantial, particularly at medium and soft sites.

Soil nonlinearity is closely linked with the level of excitation, and the type and depth of soil deposit, and, broadly speaking, can affect the seismic threat to structures in two ways. Firstly, the incident motion can be characteristically modified in terms of amplitude and frequency content. Secondly, the excitation can cause ground failure resulting in the loss of support. The present investigation is concerned with the first type of seismic effect. As the level of excitation increases, the stiffness degradation effectively results in elongation of site period [9]. Consequently, the long period components tend to play increasingly dominant role in ground response [2]. Recognition and evaluation of such effects are essential for the assessment of hazards and risks related seismic microzonation.

INCIDENT RESPONSE SPECTRA AND COMPATIBLE MOTIONS

The incident motion is characterized by defining the appropriate response spectra at stiff sites. Three levels of incident motion response spectra considered here correspond to the *frequent*, *medium*, and *extreme* levels of excitation defined for the seismic microzonation case study of Sendai area [2], and are shown in Fig. 1. In Japan, the Ohsaki standard spectra defined in the period range 0.02 to 2.0 seconds forms part of the recommendations for nuclear power plant design. The response spectra in Fig. 1 are defined to include relatively long periods of up to 10 seconds by considering a combination of Ohsaki standard spectra, and the estimation based on the prediction of large earthquakes from seismograms of small earthquakes, by the so called empirical Green's function method [1]. The small earthquake records from the dense strong motion observation array system in Sendai are utilized for this purpose.

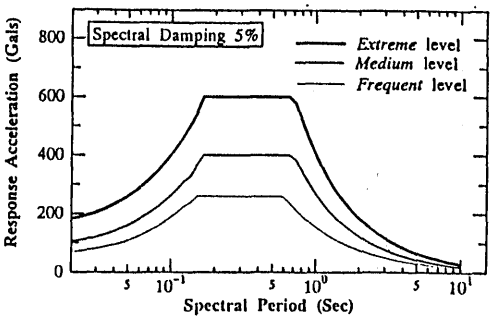

Figure 1: Incident Motion Spectra

Response spectra compatible time histories are generated by a two step iterative scheme, first in frequency domain, and then in time domain. Artificial earthquake time histories are initially generated to match approximately the response spectra in Fig. 1 based on the Equation:

$$a(t) = E(t) \times \bar{a}(t) = E(t) \times \sum_{j=1}^{M_c} \mathrm{m}_j \cos(\omega_j t - \psi_j) \tag{1}$$

Here, M_c is the number of control period points satisfying the condition given by Equation 2 [8], and $E(t)$ is the envelop function given by Equation 3 defining the overall character of the ground motion in time domain. The total durations T_D of the respective incident motions are based on the nuclear power plant design practice in Japan. The parameters of the envelop function in Equation 3 are shown in Table 1.

Table 1: Parameters of Envelop Function.

Level	T_D	t_1	t_2	C
Frequent	30.0	5.0	16.0	0.164
Medium	40.0	5.0	20.0	0.115
Extreme	52.0	4.0	24.0	0.082

$$M_c > \frac{1}{2\xi} \ln\left\{\frac{f_c}{f_o}\right\} \tag{2}$$

$$E(t) = \begin{cases} \left(\frac{t}{t_1}\right)^2, & \text{for } t \le t_1 \\ 1, & \text{for } t_1 < t \le t_2 \\ e^{-C(t-t_2)}, & \text{for } t_2 < t \le T_D \end{cases} \tag{3}$$

Utilizing the close relation between the Fourier spectra amplitude and the response spectral velocity ordinates, m_j in Equation 1 are initially replaced by spectral velocity ordinates $S_v(\omega_j)$ at the corresponding control frequencies ω_j of the target response spectra

in Fig. 1, giving the initial time history $a(t)$ from Equation 1 for subsequent iterations. The phase angles ψ_j are assumed to vary uniformly between 0 and 2π, and uniform random numbers generated in the range (0.0, 1.0) are utilized for this purpose. The response spectral ordinates of $a(t)$ calculated at the M_c control period points are compared with the corresponding target spectral ordinates. The discrete Fourier amplitudes $\mathbf{m_j}$ in Equation 1 are then modified by multiplying by the ratio between the target and the calculated spectral ordinates. This iterative scheme for modification of the time history is continued until a reasonable level of matching is achieved.

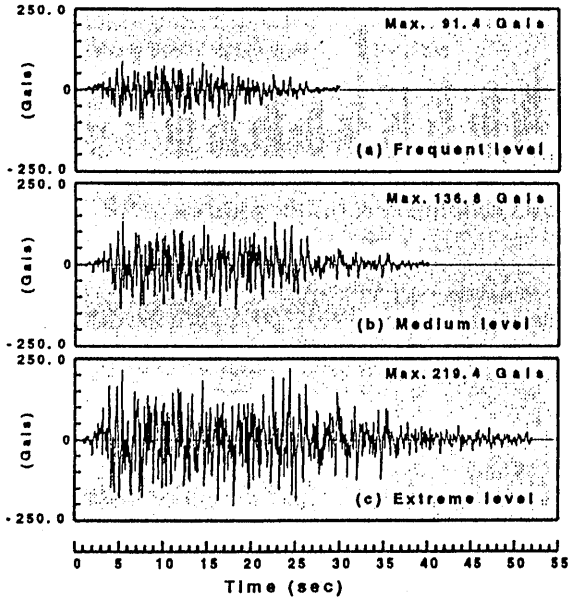

Figure 2: Three levels of incident motion time histories

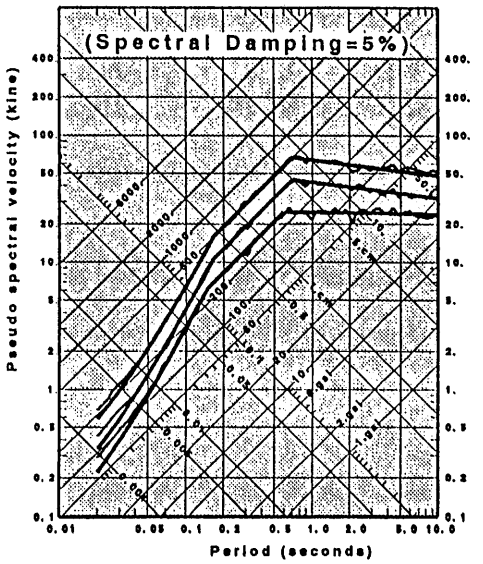

Figure 3: Compatibility of incident motions to target spectra

The time domain iterative scheme of *localized perturbation* [2, 4] in the time history at the end of frequency domain iterations is utilized to achieve a closer compatibility to the respective target response spectra. The three levels of incident motion time histories are shown in Fig. 2. The extent of compatibility to the corresponding target spectra can be seen in Fig. 3. The time domain iterative scheme is remarkable in achieving the desired extent of compatibility of the time histories initially generated based on the frequency domain iterations discussed above.

NONLINEAR RESPONSE ANALYSIS

Selection of Soil Profiles for Investigation

The ground profiles from Sendai are used in this investigation. Altogether 336 soil profiles are analized. The shear wave velocity for different soil types is estimated from the correlation of initial shear modulus G_0 with standard penetration test N–values, G_0=1200×$N^{0.8}$ (t/m^2) [7]. The soft rock underlying the Sendai area is assumed to be the base layer. Sites are assumed to be horizontally layered, and the soil profiles are modeled as a series of lumped masses connected by shear springs and dashpots. The fundamental ground period T_G of each site is computed from the mass matrix, and the stiffness matrix based on the initial shear modulus G_0 of the lumped mass model.

The sites are classified Table 2 shows site classification into six groups of different T_G ranges [10]. The corresponding classification recommended in the Japanese code for earthquake resistant design of buildings is also shown.

Table 2: Site classification and data content.

Soil *Group*	T_G range used for grouping	No. of data	Grouping in Japanese code
1	$T_G \leq 0.20$	193	1 (Hard)
2	$0.2 < T_G \leq 0.35$	67	2 (Medium)
3	$0.35 < T_G \leq 0.55$	41	
4	$0.55 < T_G \leq 0.75$	26	
5	$0.75 < T_G \leq 1.00$	8	3 (Soft)
6	$1.00 < T_G$	1	

The stiffness of soil layers during the inelastic time domain response was determined by the hysteretic model. The dependence of the shear modulus, and the equivalent damping factor, is based on the Masing's type Model developed by Ohsaki *et al.* [6]. The soil types in the selected soil profiles are broadly divided into three types: (a) clayey soils, (b) sandy soils, and (c) sandy gravel.

Nonlinear Response Analysis

The hysteretic model parameters α, β, and G_0/S_u, for the three soil types, are shown in Table 3. The corresponding shear stress-strain hysteretic plots, for a simple sinosoidal strain history with increasing amplitude, are shown in Fig. 3.

Table 3: Hysteretic model parameters

$$\epsilon = \frac{\tau}{G_o}\left\{1 + \alpha\left|\frac{\tau}{S_u}\right|^{\beta}\right\}$$

$$\xi = \frac{2}{\pi}\frac{\beta}{2+\beta}\left(1 - \frac{1}{1+\alpha\left|\frac{\tau}{S_u}\right|^{\beta}}\right)$$

ϵ = Shear Strain
τ = Shear Stress
G_o = Initial Modulus
S_u = Shear Strength
ξ = Damping Factor
$\frac{G_o}{S_u}$ = Soil Constant
α, β = Soil Constants

Soil Types	α	β	$\frac{G_o}{S_u}$
Clayey soils	5.0	1.4	600.0
Sandy soils	10.0	1.8	1200.0
Sandy gravel	12.0	1.7	1300.0

The constants of the hysteretic model for *clay* and *sand* are as given by Ohsaki *et al.* [6], and that for *gravel* is arrived at by interpolation. The nonlinear time domain response analysis is carried out by step-by-step numerical integration using the Wilson's θ-method developed by Ohsaki [5]. Viscous damping of 3% is assumed to represent damping in soil at initial conditions. The input motion is assumed to be incident at an exposed surface of base layer by considering a transmitting boundary [5].

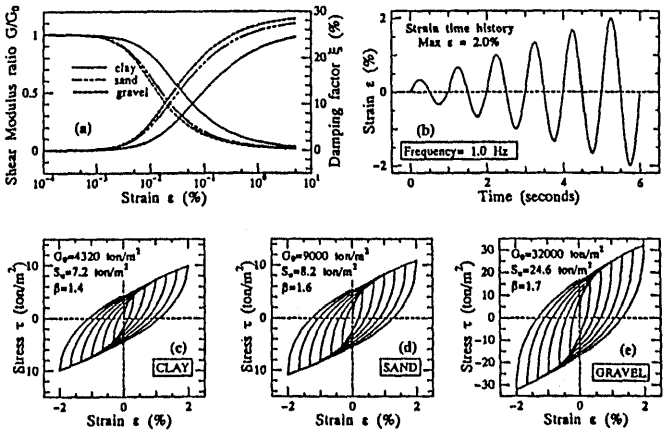

Figure 4: (a) Shear modulus and damping factors, (b) Sinosoidal strain history, and hysteretic plots for (c) *Clay*, (d) *Sand*, and (e) *Gravel*.

RESULTS OF THE INVESTIGATION

Maximum Surface Acceleration

A section across ground in Sendai is shown in Fig. 5. Distribution of maximum surface response accelerations, corresponding to the *frequent, medium*, and *extreme* levels of incident motions, are also shown. The dotted line is the fundamental ground period T_G of sites. For a given incident motion, the maximum surface acceleration is seen to decrease towards the bay area, due to increased nonlinearity at medium and soft sites [9].

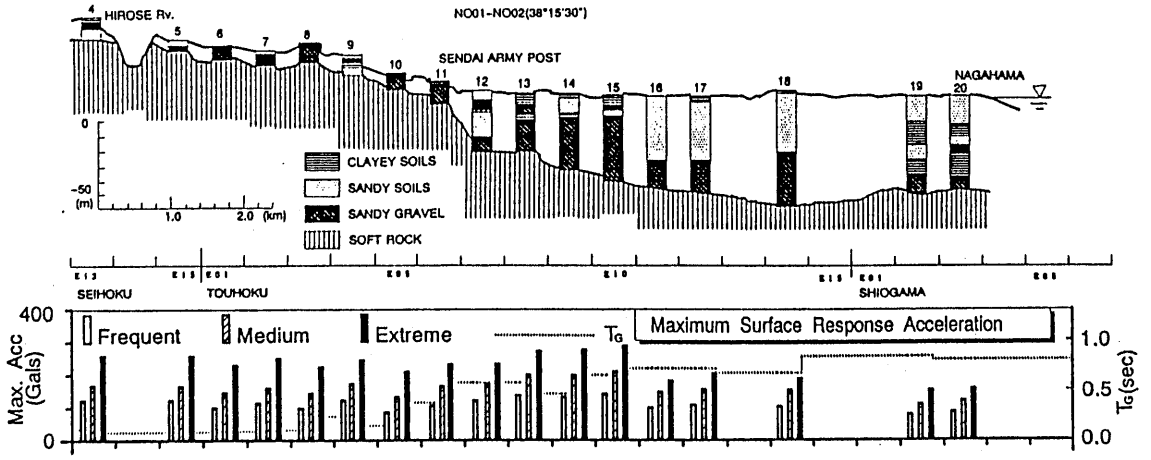

Figure 5: Sites along ground section and the distribution of maximum surface acceleration.

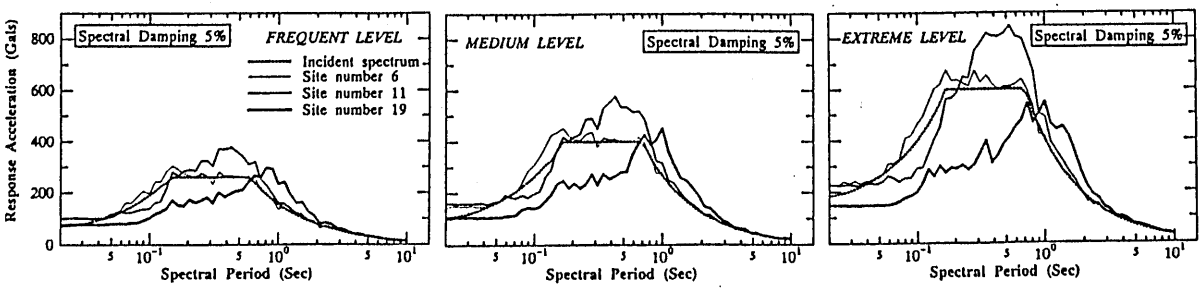

Figure 6: Surface response spectra at *stiff, medium*, and *soft* sites compared with incident motion response spectrum corresponding to (a) *frequent*, (b) *medium*, and (c) *extreme* earthquakes.

Response Spectra of Surface Response

Fig. 6 shows the response spectra of surface response corresponding to the three incident motions in Fig. 2. Response spectra at three of the sites, numbered 6, 11, and 19 in Fig. 5, representing *stiff, medium*, and *soft* sites respectively, are compared, together with the incident motion response spectra, in each case. The incident motion response spectra are modified least by the *stiff* site, particularly at lower level of excitation. The response spectra are very significantly modified by the *medium* and *soft* sites, characterized by increased dominance of long period components with the level of excitation.

Average Response Spectra

Following the method utilized for seismic microzonation study of Tokyo [10], the ground conditions are classified into six groups in Table 2. It is noted from Table 2 that most of the bore-hole data used in this investigation are from stiff sites. Attempt is made to develop site dependent response spectra for each group of sites represented by mean plus one standard deviation of the ordinates. Fig. 7 shows one such response spectra for group 3 sites, where it is seen that the response spectral ordinates all the way up to about 3.0 seconds are affected by sites in this group.

CONCLUSIONS

The effect of the different levels of excitation on the nonlinear response of different site conditions is investigated. The effect of the increase in the level of excitation on the spectral characteristics of the incident motion is noted to be dependent on the site conditions as well as on the level of excitation. There is clear indication that the level of excitation tends to stand out as an independent variable in the nonlinear response of medium and soft sites. The increasing domination of the long period components shows the need to give adequate consideration to the long period components in defining the incident motion for seismic microzonation.

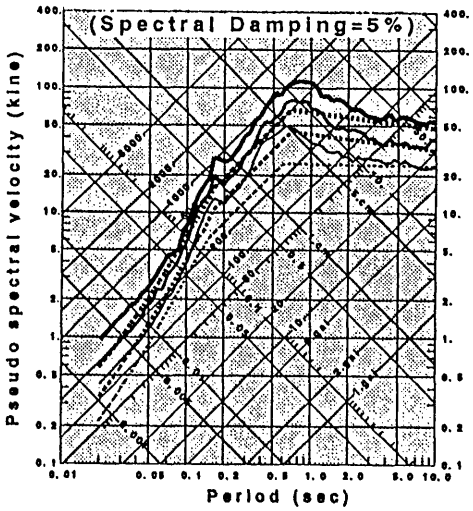

Figure 7: Site dependent spectra for group 3 sites in Table 2

References

[1] Irikura, K. and Aki, K., "Scaling law of seismic source spectra and empirical Green's function for predicting strong ground motions," *Transactions of the American Geophysical Union*, 66(967), 1985.

[2] Karkee, M. B., *Seismic Microzonation of Urban Areas Considering the Level of Excitation and the Local Soil Nonlinearity*, Doctoral Dissertation, Tohoku University, Japan, 1993.

[3] Karkee, M. B., Sugimura, Y. and Tobita, J., "Scaling a suite of ground motions for compatible levels of nonlinear ground ground response," *Journal of Structural and Construction Engineering, Tran. Architectural Institute of Japan (AIJ)*, October 1992, No. 440, pp 29–42.

[4] Lilhanand, K. and Tseng, W. S., "Development and Application of Realistic Time Histories Compatible with Multiple Damping Design Spectra," *Ninth WCEE*, 1988, pp 819–824.

[5] Ohsaki, Y., *Dynamic Nonlinear Model and One Dimensional Nonlinear Response of Soil Deposits*, Research Report 82-02, Dept. of Architecture, University of Tokyo, 1982.

[6] Ohsaki, Y., Hara, A. and Kiyota, Y., "Stress-strain Model of Soils for Seismic Analysis," *Proc. Fifth Japan Earthquake Engg. Symposium*, 1978, pp 697–704.

[7] Ohsaki, Y. and Iwasaki, R., "On dynamic shear modulii and Poisson's ratio of soil deposits," *Soils and Foundations*, Vol. 13, No. 4, 1973, pp 61–73.

[8] Preumont, A., "The generation of spectrum compatible accelerograms for design of nuclear power plants," *Earthquake Engineering and Structural Dynamics*, Vol. 12, 1984, p 481–497.

[9] Sugimura, Y., Karkee, M. B. and Ohkawa, I., "Dependence of Free Field Ground Response on Intensity of Excitation Considering Nonlinear Behavior," *Proc. Fourth International Conference on Seismic Zonation, Stanford, California*, Vol. II, 1991, pp 213–220.

[10] Sugimura, Y., Ohkawa, I. and Sugita, K., "A Seismic Microzonation Map of Tokyo," *Third International Earthquake Microzonation Conference, Seattle*, Vol. III, 1982, pp 1439–1450.